High-spin states in ^{48}V, ^{51}Cr, and ^{51}Mn

J. A. Cameron, D. G. Popescu,* and J. C. Waddington
Tandem Accelerator Laboratory, McMaster University, Hamilton, Ontario, Canada L8S 4K1
(Received 20 June 1991)

The reactions ^{40}±Ca+^{14}N at $E_N = 40$ MeV and ^{27}Al+^{27}Al at $E_{Al} = 90$ MeV are used to populate high-spin levels in a number of $f_{7/2}$ nuclei, from ^{45}Sc to ^{52}Fe. In ^{51}Cr, the $f_{7/2}$ band-terminating state at $J^{\pi} = \frac{23}{2}^-$ is identified at 5.711 MeV, and further transitions, from the pf band, are found. Similar evidence for interband transitions in ^{51}Mn is sought without success. In ^{48}V, new transitions are found within the positive-parity band and between the negative- and positive-parity bands.

I. INTRODUCTION

Low-lying states of nuclei near $A = 50$ are well described by a shell model in which $(A - 40)$ nucleons occupy the $f_{7/2}$ shell outside an inert ^{40}Ca core [1]. Such a model has interesting properties. In addition to the mirror symmetry expected from a charge-symmetric nuclear force, cross-conjugate symmetry also follows. Nuclei with $(Z,N) = (20+z, 20+n)$ and $(Z',N') = (28-n, 28-z)$ have identical spectra and simply related electromagnetic properties. A further important property of such a closed model is the existence of a single maximally spin-aligned state (band-terminating state), with $J_{\max} = J_{p\,\max} + J_{n\,\max} = [z(8-z) + n(8-n)]/2$. Indeed there is also only a single state with $J = J_{\max} - 1$. States with $J > J_{\max}$ can only be formed by excitations outside the $f_{7/2}$ shell, either from the underlying sd shell or from the higher pf shell. Because of the very large configuration space involved for a completely general treatment of such excitations, two simplified schemes have been used. In the first, only the nearest subshells, $d_{3/2}$ and $p_{3/2}$, are considered and any number of particle-hole excitations are allowed, while in the second the full sd and pf shells are opened but only small numbers of particle-hole excitations are allowed [2–4]. In addition to producing states with $J > J_{\max}$, such configurations are central to understanding spectra and transitions near $J_{\max}$ since they also form states with $J < J_{\max}$ which may mix with the $(f_{7/2})^{z+n}$ states.

The experimental situation in the $f_{7/2}$-shell nuclei ^{40}Ca to ^{56}Ni may be summarized as follows. Only for single closed shell nuclei (Z or $N = 20$ or 28) have states been observed with $J > J_{\max}$ since for these cases $J_{\max}$ is not large ($J_{\max} = 8$ for ^{44}Ca, ^{52}Cr). In few other cases has $J_{\max}$ been equaled, and never exceeded, in spite of the fact that much heavy-ion reaction spectroscopy has been done.

Two difficulties have hampered such investigations. The high excitation energy of high-spin states, roughly characterized by a moment of inertia parameter $\hbar^2/2\mathcal{J} = 0.060$ MeV near $A = 50$, about 90% of the rigid-sphere value, places states of $J_{\max}$ near or above the nucleon separation energy in many cases. The high energy of the states and therefore the large transition energies imply short lifetimes and large Doppler shifts in heavy-ion reactions. The second major difficulty is that target and projectile nuclei have small radii ($R_1 + R_2 = 6$–6.5 fm) so the angular momentum available is limited to about 40$\hbar$. Further, above about 20$\hbar$, the cross section is dominated by inelastic events rather than fusion [5] so it is difficult in the fusion-evaporation reactions to reach very far above the critical angular momentum $J_{\max}$ near midshell ($J_{\max} = 16$ for ^{48}Cr). The nuclei chosen for this study were near $A = 50$, from compound nuclei ^{54}Co and ^{54}Fe. In almost all the residue nuclei, the scheme of low-lying states has been well worked out, so residue identification and level scheme extension could be approached with confidence.

These experiments provide a foundation for attempts to find exotic deformation in lighter nuclei at high spins.

II. EXPERIMENTAL

The compound nuclei ^{54}Co and ^{54}Fe were populated, respectively, by the reactions ^{40}Ca + ^{14}N and ^{27}Al + ^{27}Al at c.m. energies of 30 and 45 MeV, respectively, chosen to optimize the three-nucleon exit channel yield yet to bring in sufficient angular momentum to populate states near $J_{\max}$. Beams of 40-MeV ^{14}N and 90-MeV ^{27}Al from the McMaster University FN Tandem accelerator bombarded 1-mg/cm^2 elemental Ca and Al targets on ^{208}Pb backings. For the Ca+N experiment, an array of five Ge detectors and a NaI multiplicity filter were used, while for the Al+Al experiment only three Ge detectors, all at 90°, were used with the filter. Coincidences were recorded in event mode.

Angular distribution measurements were carried out for both reactions in multiplicity-gated singles mode, using one Ge counter at 0°, 30°, 45°, 60° and 90°, and a second fixed at −90°. Because of the large initial recoil velocities, angular distribution data forward of 45° were difficult to analyze for the short-lived states, but gave useful information on average feeding times (from fusion to decay) for these states, from the attenuation factors F, the ratio of the measured Doppler shifts with the lead-backed target to their calculated thin target values.

Relative efficiencies of the detectors were found using standard radioactive sources.

III. RESULTS

Table I lists the residual nuclei observed. The theoretical calculations were made using the programs CASCADE [6] and PACE [7] and are in fair agreement with experiment. It is a curious fact that each of the two codes overestimates the low-A yields for only one reaction, the former for Ca+N and the latter for Al+Al. The programs moreover do not allow for inelastic entrance channel effects whereby much of the cross section at high angular momentum is lost. Figure 1 is a projection of the γ-γ matrix for the Al+Al reaction, while Figs. 2(a), 2(b), and 2(c) illustrate the selectivity of coincidences for ^{48}V, ^{51}Cr, and ^{51}Mn, respectively. Each is a summation of coincidence spectra from the Ca+N reaction gated by strong well-known transitions [8,9]. In addition to the strong peaks of the yrast cascade, in each case there are a number of weaker transitions. The Doppler broadening of the higher transitions is evident. Gates set on peaks of unknown origin allowed most to be placed in the level schemes shown in Figs. 3-5.

Only in ^{48}V and ^{51}Cr were new transitions found, feeding directly into the top of the known yrast cascades. Angular distributions of the more intense lines are summarized in Table II. Although the uncertainties are large, principally due to the loss of precision at forward angles because of the large Doppler broadening, as Fig. 6 illustrates, it is possible to assign spins to a number of new levels, shown in Figs. 3 and 4.

The effective lifetimes for levels in ^{51}Cr shown in Fig. 4 were derived from the attenuation of the Doppler shifts with angular distributions measured in multiplicity-gated singles mode and therefore do not represent individual state lifetimes. The 1.331-MeV transition from the 6.893-MeV level was observed only in coincidence, as a narrow line [see Fig. 2(b)], allowing a lower limit of about 3 ps to be set on its effective lifetime. The attenuations F of 0.2 and 0.6 for the Doppler shift of the 1.894- and 0.636-MeV transitions may be attributed to effective lifetimes of 1.7 and 0.4 ps for the $\frac{23}{2}^-$ and $\frac{19}{2}^-$ states. The fast feeding of the $\frac{19}{2}^-$ state comes through unobserved side-feeds. The slower feeding of the 0.925-MeV transition, after allowing for the 0.636-MeV cascade, together with the apparent absence of side-feeding, implies a lifetime of 0.6 ps for the 3.181-MeV $\frac{17}{2}^-$ state. The uncertainties are estimated to be about 30–50 %, mostly arising from unknown side-feeding.

IV. DISCUSSION

Almost all of the transitions found in previous heavy-ion studies of ^{48}V, ^{51}Cr, and ^{51}Mn were seen in this work. This is also even true of the more weakly populated residues such as ^{49}V, ^{49}Cr, and ^{50}Cr. In those cases, no new transitions were found. The three major residues are treated below.

TABLE I. Residue yields.

	^{40}Ca+^{14}N→^{54}Co*			^{27}Al+27Al→^{54}Fe*		
	Exp.	CASCADE	PACE	Exp.	CASCADE	PACE
^{42}Ca					6	47
^{44}Ca					0.3	8
^{44}Sc		1	1			26
^{45}Sc				80	82	67
^{47}Sc					1	4
^{45}Ti		23	4	20	17	36
^{46}Ti				55	19	9
^{47}Ti		67	2	20	62	135
^{48}Ti	0.5			80	89	61
^{50}Ti					0.2	0.3
^{45}V		0.1				
^{46}V		0.1	1.6			
^{47}V		25	0.5	10	5	36
^{48}V	45	96	72	45	110	350
^{49}V	0.4			45	31	23
^{50}V		47	3	50	40	70
^{51}V					8	11
^{48}Cr	2	24	8	10	4	28
^{49}Cr	29	4	15	25	11	16
^{50}Cr	7	230	11	65	84	200
^{51}Cr	100	100	100	100	100	100
^{52}Cr				5	0.6	1.4
^{49}Mn		0.1	0.3			8
^{50}Mn	1	8	0.2		0.8	54
^{51}Mn	180	63	100	70	19	0.3
^{52}Mn	9	0.2	10	2	0.3	0.3
^{51}Fe		3	0.7		0.2	0.7
^{52}Fe	1	0.1	2			

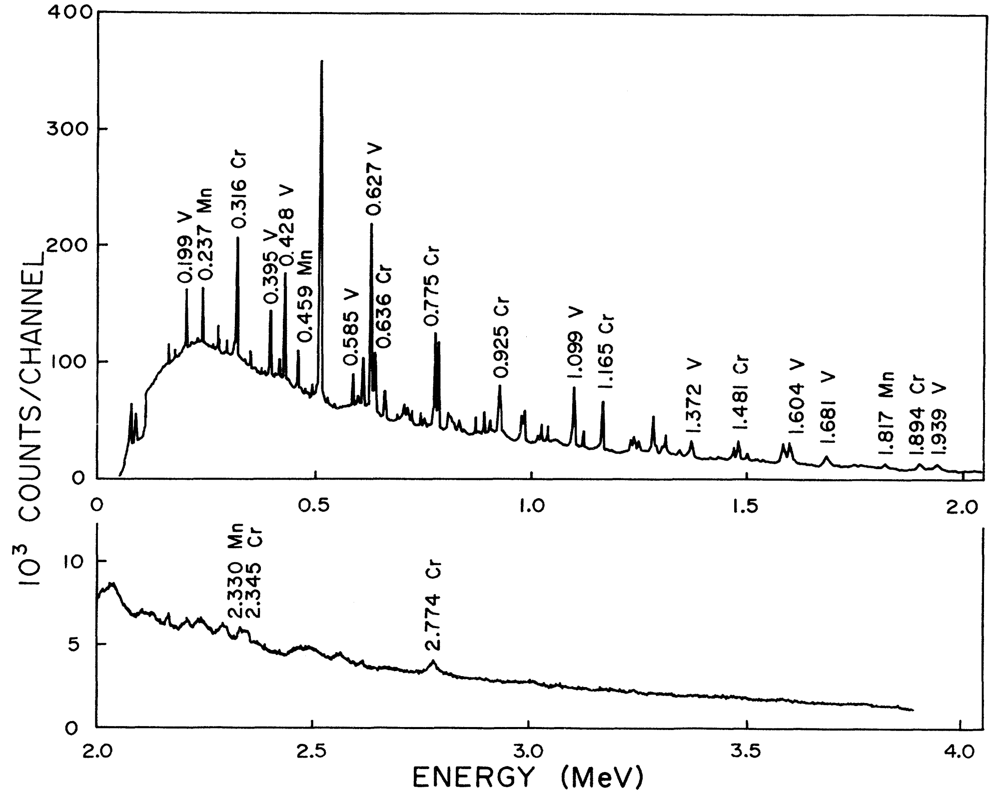

FIG. 1. Projection of the γ-γ coincidence matrix for Al+Al at 90 MeV. Strong γ rays from ^{48}V, ^{51}Cr, and ^{51}Mn are labeled.

A. ^{48}V

The positive-parity $(f_{7/2})^8$ band is yrast and so contains most of the decay strength. Reference [8] places two 8^+ levels, both connected by 0.395- and 0.977-MeV transitions to the 9^+ and 7^+ levels, but in reverse order. The lower level, at 1.650 MeV has no other feeds or decays, while the upper one, at 2.232 MeV, decays also to the 6^+ level by a weak 1.604-MeV transition. It appears that the present, and all previous experimental results may be accounted for by the presence of only the 2.232-MeV 8^+ state, indicated in Fig. 3. Although the band is expected to terminate at 15^+, no levels have previously, or in this work, been observed above the 6.241-MeV state, proposed to be 13^+. Five transitions, so far unplaced, may be connected to the expected higher levels. The dashed levels and transitions were observed only in coincidence gates below the 9^+ but may occur higher.

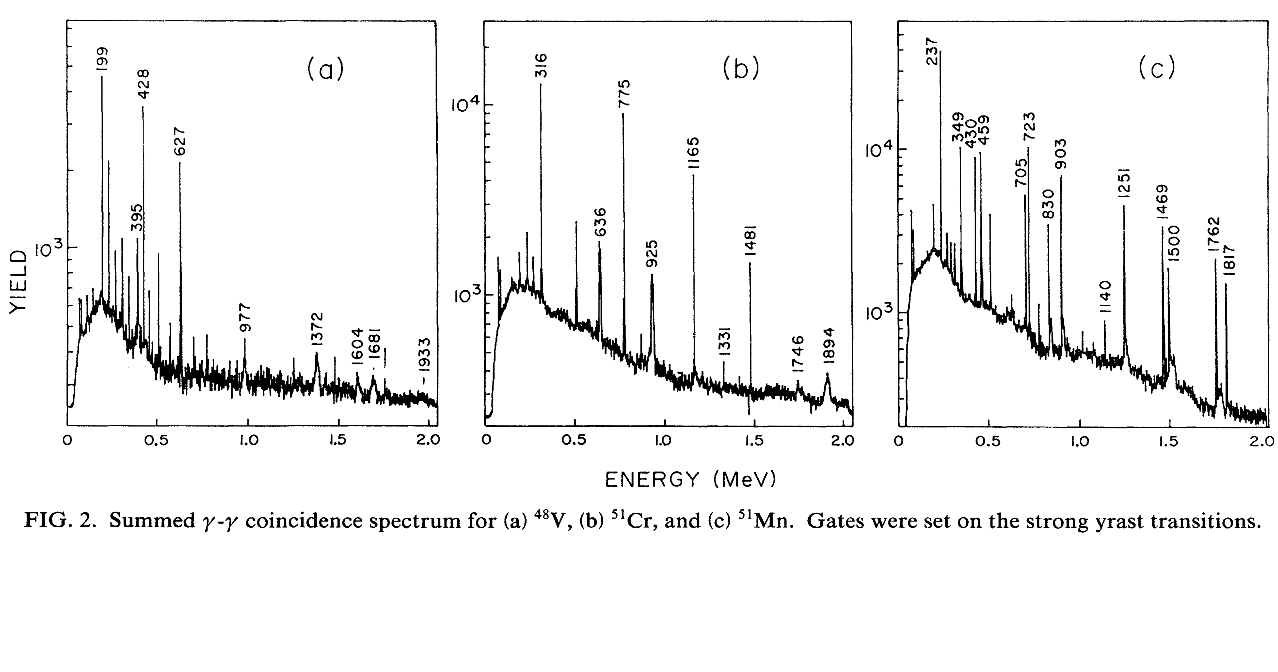

FIG. 2. Summed γ-γ coincidence spectrum for (a) ^{48}V, (b) ^{51}Cr, and (c) ^{51}Mn. Gates were set on the strong yrast transitions.

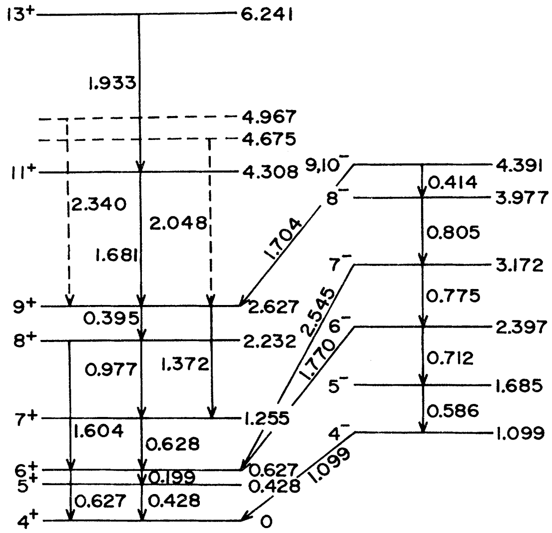

FIG. 3. Level scheme of ^{48}V based on this work.

The positive-parity levels are compared with the yrast levels of the $(f_{7/2})^8$ shell model [1] in Fig. 7.

There are in ^{48}V two negative-parity bands, based on the 1^- 0.518-MeV and 4^- 1.099-MeV levels. It has been proposed that these arise from a proton particle-hole excitation in which a $d_{3/2}$ hole is coupled to the ^{49}Cr ground state [10]. The 1^- band was not observed in this study, but the 4^- band was seen up to the 4.391-MeV level, of spin 9^- or 10^-, still far from the expected termination at 17^-. In addition, there are three weak band-connecting transitions, previously unobserved. The rela-

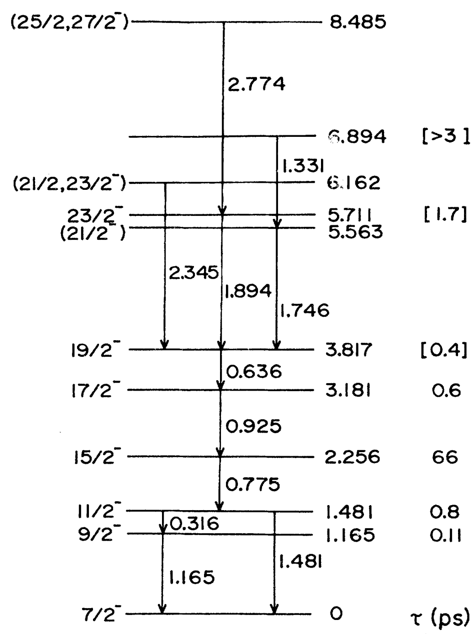

FIG. 4. Level scheme of ^{51}Cr based on this work. The bracketed times are effective lifetimes in ps for the corresponding decays.

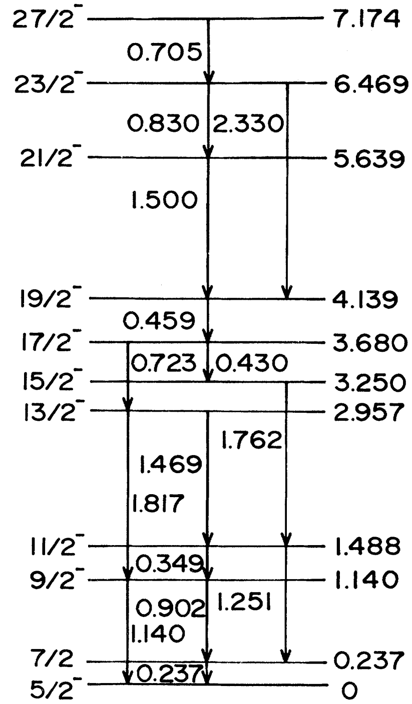

FIG. 5. Level scheme of ^{51}Mn based on this work.

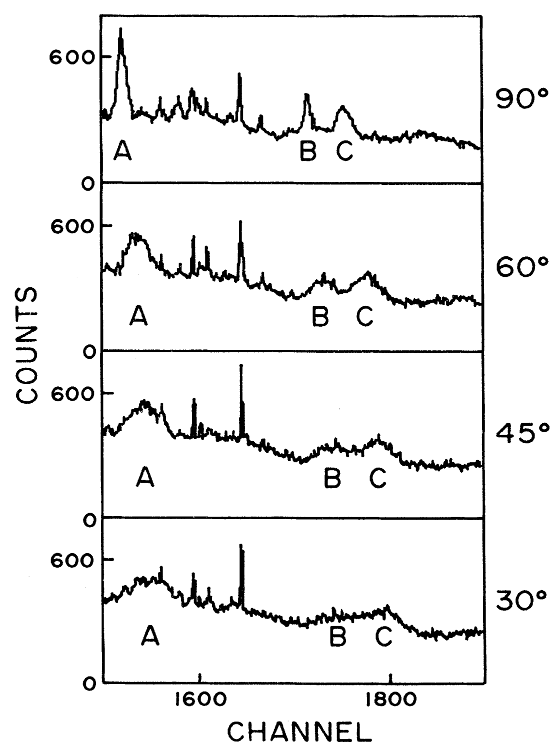

FIG. 6. Part of the multiplicity-gated singles angular distribution spectra for Ca+N. The lines A and C are from ^{48}V (1.681 and 1.936 MeV), B from ^{51}Cr (1.896 MeV).

TABLE II. Angular distributions.

^{48}V

E_i	E_γ	A_2	A_4	J_f^π	J_i^π
0.428	0.428	−0.56(10)	0.15(10)	4^+	5^+
0.627	0.199	−0.48(10)	0.01(10)	5^+	6^+
1.655	0.395	−1.3(2)	0.5(1)	7^+	8^+
2.627	1.372	−0.17(12)	0.15(12)	7^+	9^+
	0.977	−0.81(15)	0.17(14)	8^+	
4.308	1.681	0.38(10)	−0.04(12)	9^+	11^+
6.241	1.933	0.78(18)	0.04(21)	11^+	13^+

^{51}Cr

E_i	E_γ	A_2	A_4	J_f^π	J_i^π	F
1.165	1.165	−0.70(11)	0.21(9)	$\frac{7}{2}^-$	$\frac{9}{2}^-$	
1.481	1.481	0.24(9)	0.09(11)	$\frac{7}{2}^-$	$\frac{11}{2}^-$	
	0.316	−0.50(10)	0.13(9)	$\frac{9}{2}^-$		
2.225	0.775	0.20(10)	0.05(11)	$\frac{11}{2}^-$	$\frac{15}{2}^-$	
3.180	0.925	−0.35(12)	0.20(13)	$\frac{15}{2}^-$	$\frac{17}{2}^-$	0.30(5)
3.816	0.636	−0.47(12)	0.21(13)	$\frac{17}{2}^-$	$\frac{19}{2}^-$	0.62(10)
5.711	1.894	0.28(22)	−0.34(28)	$\frac{19}{2}^-$	$\frac{23}{2}^-$	0.20(4)

tive weakness of these higher-energy $E1$ transitions, compared to the low-energy in-band $M1$ decays suggests a high degree of forbiddenness in the former.

B. ^{51}Cr

The angular distribution results for ^{51}Cr allow the assignment of firm spin values of $\frac{17}{2}^-$ and $\frac{19}{2}^-$ for the already known 3.180- and 3.816-MeV levels, and $\frac{23}{2}^-$ for the newly found level at 5.711 MeV. The last is the $f_{7/2}$ band-terminating state with its spin of $\frac{23}{2}^-$. The spins shown in parentheses in Fig. 4 are inferred from decay branching only. The low intensity of the higher transitions makes angular distribution analysis impracticable but the anomalously long lifetime of the 1.331-MeV tran-

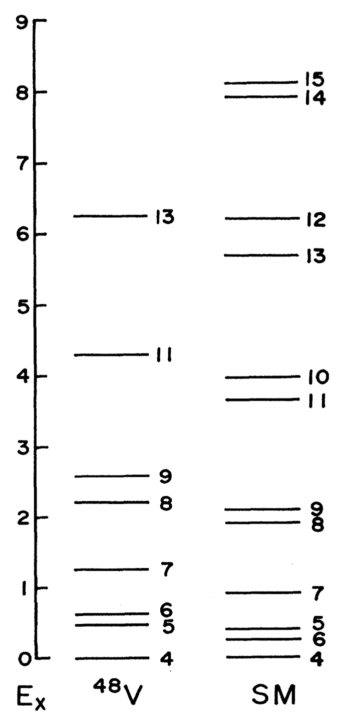

FIG. 7. Positive-parity levels of ^{48}V observed in this work compared with the $f_{7/2}$ shell model [1]. The excitation energy scale is in MeV.

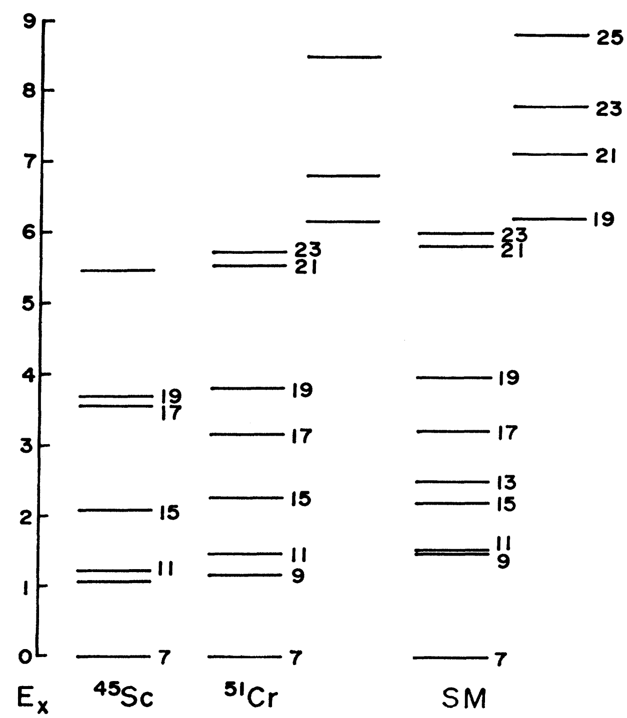

FIG. 8. Comparison of ^{51}Cr negative-parity yrast levels with those predicted by the shell model [4] and with the levels of ^{45}Sc. Spins are given as $2J$, energies in MeV.

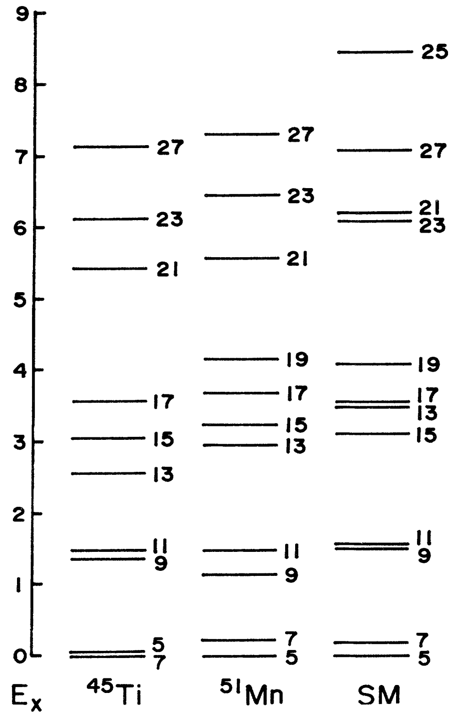

FIG. 9. Comparison of the negative-parity yrast levels of ^{51}Mn and ^{45}Ti with those predicted by the shell model [1]. Spins are given as $2J$, energies in MeV.

sition is suggestive of hindrance of an $M1$ decay $(f_{7/2})^{10}p_{3/2} \to (f_{7/2})$.[11] The other two transitions, leading to the 5.711-MeV $\frac{23}{2}^-$ level, appear to be rapid. This situation is similar to that found in ^{53}Mn near the band-terminating spin of $\frac{15}{2}^-$. There the $\frac{17}{2} \to \frac{15}{2}$ transition is slow while higher levels decay rapidly, not only to the $\frac{17}{2}$ as would be expected for in-band transitions, but to the $\frac{15}{2}$ level as well. The implication is either that the "band-terminating" state is mixed with a member of the pf band or that some members of the pf band near $J_{\max}$ contain, in addition to the expected $(f_{7/2})^{-1}p_{3/2}$ component, a strong $(f_{7/2})^{-1}f_{5/2}$ one. The presence of the slow transition in both ^{51}Cr and ^{53}Mn seems to favor the latter interpretation. Reference [4] notes that this involvement of the full pf shell in the intruder band is needed to explain the enhancement of the $E2$ transitions among the low-lying states.

Figure 8 compares the levels found in the present work with those predicted from the shell model including $(f_{7/2})^{11}$ and $(f_{7/2})^{10}(p_{3/2}f_{5/2}p_{1/2})^1$ configurations [4].

C. ^{51}Mn

In spite of the strength of the ^{51}Mn yrast cascade observed in both reactions, no further transitions were seen in the individual or summed coincidence spectra. We therefore conclude that little strength leads to levels with $J > J_{\max} = \frac{23}{2}$. If this is so, it suggests that the upper angular momentum limit for compound nucleus formation is somewhat lower than theory predicts [5]. Of the transitions among the lower, well-known, levels, only the crossover 2.331-MeV decay $\frac{23}{2}^- \to \frac{19}{2}^-$ was previously unreported . The $\frac{15}{2}^- \to \frac{13}{2}^-$ 0.293-MeV transition was not seen. The level scheme is compared with the yrast states of the $(f_{7/2})^{11}$ shell model in Fig. 9.

D. ^{45}Sc, ^{45}Ti

It is of interest to compare the level schemes of ^{51}Cr and ^{51}Mn with those of their $f_{7/2}$ cross conjugates ^{45}Sc and ^{45}Ti. These were populated in the $2\alpha p$ and $2\alpha n$ exit channels in the Al+Al reaction. The former was not a strong branch. No new transitions were found in ^{45}Ti, but the 0.981-MeV decay of the supposed $\frac{27}{2}^-$ level [11] was confirmed. No evidence was found for the known $\frac{9}{2}^-$ level at 1.354 MeV, nor for a $\frac{19}{2}^-$ level, presently unknown but expected, on the basis of cross-conjugate symmetry, between 4.0 and 4.2 MeV. In ^{45}Sc, there is a candidate for the $\frac{9}{2}^-$ level expected near 1.0 MeV, but no spin assignment has been made. The 5.419-MeV level is thought to be $\frac{21}{2}^-$ or $\frac{23}{2}^-$. As Figs. 8 and 9 show, the cross-conjugate symmetry is well kept for the high-spin states. This contrasts with its failure for the $\frac{3}{2}^-$ and positive-parity states [9,11], which are strongly influenced by out-of-shell excitations.

V. CONCLUSIONS

The present experiments confirm the expectation that the high-spin band in ^{51}Cr continues beyond the maximum spin allowed within the $f_{7/2}$ shell and give evidence of both fast and slow transitions into the lower-spin states. This is the first observation in non-closed-$f_{7/2}$-shell nuclei of states beyond $J_{\max}$. Further transitions were found in ^{48}V, leading to the highest known levels in the positive-parity band and joining the negative- and positive-parity bands.

ACKNOWLEDGMENTS

The authors are grateful to colleagues at the Australian National University, the University of Manchester, and Daresbury Laboratory for helpful discussions, and to the Natural Sciences and Engineering Research Council of Canada and the Science and Engineering Research Council of Great Britain for financial support.

*Present address: Institut de Physique Nucléaire, Université Paris-Sud, 91406 Orsay, France.

[1] W. Kutschera, B. A. Brown, and K. Ogawa, Riv. Nuovo Cimento Ser. 3, **1**, 1 (1978).
[2] A. Poves and A. Zuker, Phys. Rep. **70**, 235 (1981).
[3] L. Zybert, P. W. Glaudemans, R. B. M. Mooy, and D. Zwarts, Z. Phys. A **318**, 363 (1984).
[4] A. Yokoyama and H. Horie, Phys. Rev. C **31**, 1012 (1985).
[5] R. Bass, *Nuclear Physics with Heavy Ions* (Springer-Verlag, Berlin, 1980).
[6] F. Pühlhofer, Nucl. Phys. A **280**, 267 (1977).
[7] A. Gavron, Phys. Rev. C **21**, 230 (1980).
[8] D. E. Alburger, Nucl. Data Sheets **45**, 557 (1985).
[9] Zhou Chunmei, Zhou Enchen, Lu Xiane, and Ho Junde, Nucl. Data Sheets **48**, 111 (1986).
[10] M. Morando *et al.*, Phys. Lett. **64B**, 140 (1976); in *Proceedings of the International Conference on Medium-Light Nuclei,* Florence, Italy, 1977, edited by P. Blasi and R. A. Ricci (Compositori, Bologna, 1978), p. 468.
[11] T. W. Burrows, Nucl. Data Sheets **40**, 149 (1983).